PHILOSOPHICAL TRANSACTIONS A

rsta.royalsocietypublishing.org

Research

Cite this article: Žunkovič B, Silva A, Fabrizio M. 2016 Dynamical phase transitions and Loschmidt echo in the infinite-range XY model. *Phil. Trans. R. Soc. A* **374**: 20150160. http://dx.doi.org/10.1098/rsta.2015.0160

Accepted: 22 December 2015

One contribution of 12 to a theme issue 'Loschmidt echo and time reversal in complex systems'.

Subject Areas:
statistical physics, quantum physics

Keywords:
non-equilibrium, quantum phase transitions, Loschmidt echo

Author for correspondence:
Alessandro Silva
e-mail: asilva@sissa.it

Dynamical phase transitions and Loschmidt echo in the infinite-range XY model

Bojan Žunkovič[1,2], Alessandro Silva[2] and Michele Fabrizio[2]

[1]Departamento de Física, Facultad de Ciencias Físicas y Matemáticas, Universidad de Chile, Casilla 487-3, Santiago, Chile
[2]Scuola Internazionale Superiore di Studi Avanzati (SISSA), Via Bonomea 265, Trieste, Italy

AS, 0000-0002-5668-7134

We compare two different notions of dynamical phase transitions in closed quantum systems. The first is identified through the time-averaged value of the equilibrium-order parameter, whereas the second corresponds to non-analyticities in the time behaviour of the Loschmidt echo. By exactly solving the dynamics of the infinite-range XY model, we show that in this model non-analyticities of the Loschmidt echo are not connected to standard dynamical phase transitions and are not robust against quantum fluctuations. Furthermore, we show that the existence of either of the two dynamical transitions is not necessarily connected to the equilibrium quantum phase transition.

1. Introduction

Recent experiments with cold atoms in optical lattices [1], ion traps [2] and ultrafast pump-probe spectroscopy [3] have triggered a lot of interest in the study of the dynamics of thermally isolated many-body systems. In both classical and quantum physics, isolated systems have the peculiarity of displaying a dynamics that is very sensitive to the type of interactions among their constituents. In particular, a generic non-integrable system is expected to behave ergodically (hence thermalize after being kicked out of equilibrium), whereas an integrable system is not [4]. In addition, a quantum

THE ROYAL SOCIETY PUBLISHING

many-body system taken out of equilibrium by changing its parameters (i.e. by a *quantum quench*) may relax towards a thermal state passing through an intermediate long-lived non-thermal quasi-steady state.

This phenomenon, known as pre-thermalization [5,6], is expected in systems close to being either integrable [7] or mean-field like, in particular in spin chains [8,9] or perturbed Luttinger liquids [10,11].

Non-thermal states such as those associated with pre-thermalization may display as a function of the parameters critical phenomena similar to those observed in equilibrium systems when the temperature is varied. This type of dynamical criticality should be understood as a non-analytic change of the dynamical order parameter, defined for example through the time average of the equilibrium-order parameter characterizing the corresponding quantum phase transition. Dynamical phase transitions were extensively studied in mean-field models [12–18], where, in most cases, the critical line of the dynamical phase transition is shifted towards the ordered phase w.r.t. the equilibrium quantum phase transition line. Although these transitions have a purely dynamical origin, it has been argued that the existence of the quantum phase transition is intertwined with the existence of a dynamical one [14].

In addition to this standard meaning of dynamical criticality, a second notion of criticality out-of-equilibrium has been recently introduced in the work of Heyl *et al.* [19]. It is related to the occurrence of non-analytic temporal behaviour of the dynamical free energy density, defined as the logarithm of the Loschmidt amplitude [19–21]

$$f(t) = \lim_{N\to\infty} \frac{1}{N} \ln\langle\psi|e^{-iHt}|\psi\rangle, \tag{1.1}$$

where N denotes the number of particles in the system and $|\psi\rangle$ is the initial state. This interpretation follows from the observation that the Loschmidt amplitude $G(t) = \langle\psi|e^{-iHt}|\psi\rangle$ (also known as the return probability) can be regarded as a dynamical partition sum [22,23]. It has been shown [19] that the effects of Fisher zeros in $G(t)$ can be observed in the statistics of the work done in a quantum quench protocol. Vajna & Dóra [21] showed that the existence of the dynamical transition in $G(t)$ is not related to the existence of the equilibrium phase transition in the XY spin-$\frac{1}{2}$ chain. In [24], a topological classification of the dynamical transition was suggested, and in [25] a dynamical mean-field theory was developed to describe the non-analyticities in $G(t)$.

Despite having been studied extensively in a variety of systems, the connection between the two notions of dynamical criticality has hardly been investigated. Non-analyticities in $f(t)$ (i.e. zeros in the return probability) are observed in one-dimensional systems that do not display standard dynamical criticality. It is however unclear whether the two notions might be connected in systems displaying standard dynamical critical phenomena. In order to address this question, in this paper, we consider the dynamics of the infinite-range XY model, studying both the non-equilibrium dynamics of the order parameter as well as that of the Loschmidt amplitude. We show that for certain initial states the emergence of dynamical criticality in the time-averaged-order parameter comes hand in hand with the appearance of zeros in the Loschmidt amplitude. However, while standard criticality is robust against quantum fluctuations, the zeros of the Loschmidt amplitude are not. In addition, a study of the dependence of this phenomenon on initial conditions shows that even at the strict mean-field level the two notions appear not to be related.

The rest of the paper is organized as follows. In §2, we set up the notation and review the equilibrium phase diagram of the model. In §3, we focus instead on the standard notion of dynamical criticality and derive the dynamical phase diagram. In §4, we discuss the physics of the Loschmidt amplitude, studying the connection between the two types of criticalities as well as the robustness of zeros of the Loschmidt amplitude towards quantum fluctuations. Finally, in §5, we present our conclusions.

2. Infinite range XY model—zero temperature phase diagram

In the following, we study the dynamics of the infinite range XY model,

$$H = -\frac{2}{N}\sum_{i<j}^{N}\left(\frac{1+\gamma}{2}\sigma_i^{\mathrm{x}}\sigma_j^{\mathrm{x}} + \frac{1-\gamma}{2}\sigma_i^{\mathrm{y}}\sigma_j^{\mathrm{y}}\right) - h\sum_{i=1}^{N}\sigma_i^{z}, \tag{2.1}$$

where σ_j^a, with $a \in \{\mathrm{x},\mathrm{y},\mathrm{z}\}$, denote the Pauli matrices at site j. By using the definition $S^a = \frac{1}{2}\sum_{j=1}^{N}\sigma_j^a$, the Hamiltonian can be rewritten as a spin $S = N/2$ model,

$$H = -\frac{4}{N}\left(\frac{1+\gamma}{2}(S^{\mathrm{x}})^2 + \frac{1-\gamma}{2}(S^{\mathrm{y}})^2\right) - 2hS_i^z. \tag{2.2}$$

In the large spin limit, the model behaves classically and the mean-field description becomes exact. Moreover, phase-space methods become particularly useful as they permit a systematic expansion around the classical/thermodynamic limit. In the phase space, the von Neumann equation for the density matrix attains the form of a partial differential equation for a quasi-probability distribution, which may be obtained by using the formalism of Bopp operators (or D-algebras) [26]

$$\left.\begin{aligned}\partial_t W^{(s)} &= -\partial_{\boldsymbol{m}}\cdot(\boldsymbol{m}\times\boldsymbol{B})W^{(s)} + \mathcal{O}\left(\frac{1}{S^2}\right)\\ \text{and}\qquad \boldsymbol{B} &= (2(1+\gamma)m_{\mathrm{x}}, 2(1-\gamma)m_{\mathrm{y}}, 2h),\end{aligned}\right\} \tag{2.3}$$

with $\boldsymbol{m}(\theta,\varphi) = (\sin\theta\cos\varphi, \sin\theta\sin\varphi, \cos\theta)$. The Weyl symbol is defined through the quantization kernel $W^{(s)}(\theta,\phi,t) = \mathrm{tr}\rho(t)K^{(s)}(\theta,\phi)$, where the parameter s denotes the ordering of the phase-space distribution, i.e. distinguishes between the Husimi function (for $s=-1$), Wigner function (for $s=0$) and Glauber–Sudarshan function (for $s=1$). We shall use the kernel for the Husimi function $K(\theta,\varphi) = |\theta,\varphi\rangle\langle\theta,\varphi|$, where $|\theta,\varphi\rangle$ denotes a $SU(2)$ spin coherent state [27]. We remark that in the mean-field the choice of the kernel is irrelevant, because all kernels lead to the same classical evolution. Equation (2.3) for the Husimi function can be regarded as a classical Liouville equation acting on a phase space, which is in this case a two-dimensional sphere. It can be rewritten in the standard form $\partial_t W = \{H^{\mathrm{cl}}, W\}_{\mathrm{P}}$ by defining the spin Poisson bracket

$$\{m_a, m_b\}_{\mathrm{P}} = \epsilon_{a,b,c}m_c \tag{2.4}$$

and the classical Hamiltonian

$$H^{\mathrm{cl}} = -((1+\gamma)m_{\mathrm{x}}^2 + (1-\gamma)m_{\mathrm{y}}^2 + 2hm_z), \tag{2.5}$$

where $\epsilon_{a,b,c}$ denotes the Levi–Civita tensor. The classical Hamiltonian can be further rewritten as

$$H^{\mathrm{cl}} = -(1+\gamma)(1-p^2)\cos^2 q - (1-\gamma)(1-p^2)\sin^2 q - 2hp, \tag{2.6}$$

with the canonical variables $q \in \mathbb{R}$ and $p \in [-1,1]$ defined as

$$m_{\mathrm{x}} = \cos q\sqrt{1-p^2}, \quad m_{\mathrm{y}} = \sin q\sqrt{1-p^2} \quad \text{and} \quad m_z = p. \tag{2.7}$$

The new variables, p, q, satisfy the commutation relation $\{q,p\}_{\mathrm{P}} = 1$. Each phase-space point of the probability distribution evolves in time according to the classical equations of motion,

$$\partial_t p(t) = -\partial_q H^{\mathrm{cl}} \quad \text{and} \quad \partial_t q(t) = \partial_p H^{\mathrm{cl}}, \tag{2.8}$$

and corresponds to a coherent state. The overlap between two coherent states can be obtained by considering spin S as a compositum of spins $\frac{1}{2}$ all pointing in the same direction. Hence, we have

$$|\langle\theta_1,\varphi_1|\theta_2,\varphi_2\rangle|^2 = \left(\frac{1+\boldsymbol{m}_1\cdot\boldsymbol{m}_2}{2}\right)^N. \tag{2.9}$$

The classical equations are correct up to the order $1/S^2$. This enables a calculation of the equilibrium phase diagram by finding the phase-space point that minimizes the classical

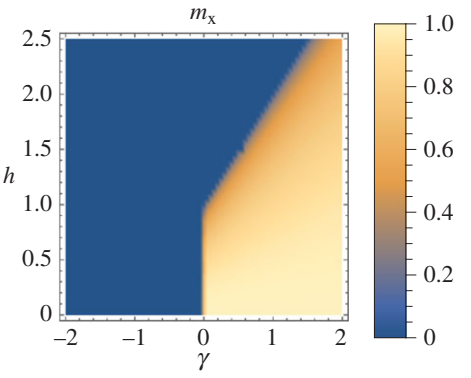

Figure 1. Mean-field zero temperature phase diagram for the order parameter $m_x = \lim_{N\to\infty}\langle 2S_x/N\rangle$. (Online version in colour.)

Hamiltonian for a given set of parameters. Throughout the paper, we shall choose the order parameter as the on-site magnetization in the x-direction. Therefore, the equilibrium phase diagram, distinguishing the disordered phase ($m_x = 0$) and the ordered one ($m_x \neq 0$), is easily obtained by calculating m_x at the minima of equation (2.5), thus obtaining figure 1.

3. Dynamical phase transition I: time-averaged order parameter

Let us now study the dynamics focusing on the long-time averages of the equilibrium-order parameter after a quantum quench, i.e. $\bar{m}_x = \lim_{t\to\infty}(1/t)\int_0^t \mathrm{d}s\, m_x(s)$. This is easily done numerically by solving classical equations of motion. For the sake of simplicity, let us first consider a sudden quench from $(\gamma_i, h_i) = (1, 0)$ to (γ_f, h_f); using $\bar{m}_x$ as the order parameter, we obtain the phase diagram shown in figure 2. In contrast to previously described dynamical transitions, we observe that the dynamical phase transition can be absent even if we cross the critical line of an equilibrium phase transition.

These results are obtained by using the energy conservation and expressing the Hamilton–Jacobi equations (2.8) as

$$\left.\begin{aligned} p &= \frac{h_f - \sqrt{h_f^2 - 2\gamma_f \sin^2(q)(\gamma_f \cos(2q) + 1)}}{\gamma_f \cos(2q) + 1} \\ \text{and} \qquad \partial_t q &= -2\sqrt{h_f^2 - 2\gamma_f \sin^2(2q)(\gamma_f \cos(2q) + 1)}. \end{aligned}\right\} \tag{3.1}$$

In this section, we use p, q instead of $p(t), q(t)$ in order to simplify the notation. The solution of equations (3.1) with the initial conditions $q(0) = p(0) = 0$ (i.e. for a quench from $(\gamma_i, h_i) = (1, 0)$) can be written in the following compact form:

$$\left.\begin{aligned} q &= \arctan\left(-\frac{K^- \mathrm{sn}(2tK^+|(K^-/K^+)^2)}{\sqrt{2(\gamma_f - 1)\gamma_f + h_f^2}}\right) \\ \text{and} \qquad K^\pm &= \sqrt{(-h_f^2 + \gamma_f^2 + \gamma_f \pm \sqrt{(\gamma_f + 1)^2 - 4h_f^2}|\gamma_f|)}. \end{aligned}\right\} \tag{3.2}$$

The dynamical phase diagram shown in figure 2 is determined by the properties of the coefficient K^+, namely $\bar{m}_x = 0 \Leftrightarrow \mathrm{Im}(K^+) \neq 0$. If $\mathrm{Im}K^+ = 0$, then q oscillates in the interval $[-q_{\max}, q_{\max}]$, where $q_{\max} = \arctan\left|K^-\Big/\sqrt{2(\gamma_f - 1)\gamma_f + h_f^2}\right| < \pi/4$, hence $\bar{m}_x > 0$. In the regime where $\mathrm{Im}K^+ \neq 0$, the angle $\mod 2\pi(q(t))$ covers the interval $[0, 2\pi]$ (owing to simple poles of the Jacobi elliptic function). Because the equation of motion is invariant under the shift $q \to q + \pi$, we see that $q(t)$

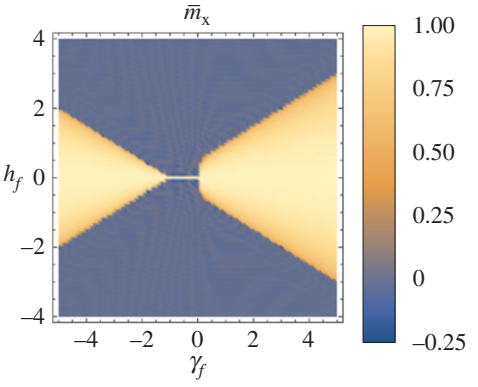

Figure 2. Dynamical phase diagram for the time-averaged order parameter $\bar{m}_x$ for a sudden quench from $(\gamma_i, h_i) = (1, 0)$ to (γ_f, h_f). The averaged order parameter $\bar{m}_y$ vanishes for any quench from $(\gamma_i, h_i) = (1, 0)$, i.e. from an m_y-paramagnetic phase. (Online version in colour.)

spends the same amount of time in the interval $[\pi/2, 3\pi/2]$ as in the interval $[-\pi/2, \pi/2]$, implying a vanishing average $\bar{m}_x = 0$.

A general solution to the Hamilton–Jacobi, equations (2.8), can be obtained by expressing the momentum p in terms of the coordinates q using the energy conservation $2\epsilon = H(\gamma_f, h_f, p_i, q_i) = H(\gamma_f, h_f, p(t), q(t))$:

$$p = \frac{h_f \pm \sqrt{h_f^2 + (\gamma_f \cos 2q + 1)(\gamma_f \cos 2q + 2\epsilon + 1)}}{\gamma_f \cos 2q + 1}. \tag{3.3}$$

The function under the square root is positive iff $|h_f| > |\epsilon|$. Next, we insert the above expression into the equation of motion for q and obtain

$$\partial_t q = \pm 2\sqrt{h_f^2 + (\gamma_f \cos 2q + 1)(\gamma_f \cos 2q + 2\epsilon + 1)}, \tag{3.4}$$

where the sign is determined by the initial condition. The solution of equation (3.4) is

$$\left.\begin{aligned} q(t) &= 2\arctan\left(\mathrm{i}\frac{\mathrm{sn}(u|m)}{n}\right), \\ u &= \frac{s}{2}\sqrt{(C_2 + t)^2(16\gamma_f^2 - C_1 + 2\sqrt{256\gamma_f^2(\epsilon+1)^2 - 16C_1\gamma_f^2})}, \\ m &= \frac{-16\gamma_f^2 + C_1 + 2\sqrt{256\gamma_f^2(\epsilon+1)^2 - 16C_1\gamma_f^2}}{-16\gamma_f^2 + C_1 - 2\sqrt{256\gamma_f^2(\epsilon+1)^2 - 16C_1\gamma_f^2}} \\ \text{and} \qquad n &= \sqrt{\frac{16\gamma_f^2 - 32\gamma_f(\epsilon+1) + C_1}{-16\gamma_f^2 + 2\sqrt{256\gamma_f^2(\epsilon+1)^2 - 16\gamma_f^2 C_1} + C_1}}, \end{aligned}\right\} \tag{3.5}$$

where $\mathrm{sn}(u|m)$ denotes a Jacobi elliptic function and the constants C_1, C_2 are determined by the initial conditions.

4. Dynamical phase transition II: zeros of the Loschmidt amplitude

The Loschmidt echo ($|G|^2$) can be calculated from equation (2.9). For the particular quench starting from $(\gamma_i, h_i) = (1, 0)$, we obtain $|G(t)|^2 = ((1 + m_x(t))/2)^N$. In this case, the dynamical phase diagram that is obtained by plotting the minimum of the Loschmidt echo with respect to time exactly agrees with the phase diagram shown in figure 2. However, this is a rather exceptional case,

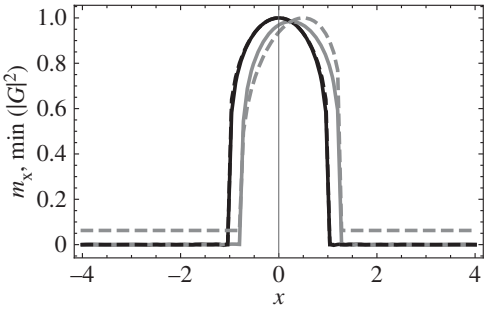

Figure 3. Minimum of the Loschmidt echo (dashed lines) and time-averaged order parameter $\bar{m}_x$. We show quenches from $(\gamma_i, h_i) = (1, 0)$ (black lines) and from $(\gamma_i, h_i) = (1, 1/2)$ (grey lines) to $(\gamma_f, h_f) = (1, x)$. For the quench from $(\gamma_i, h_i) = (1, 0)$, the black lines are on top of each other.

as can be seen from figure 3, where we show the quench from $(\gamma_i, h_i) = (1, 0.5)$ in addition to the quench from $(\gamma_i, h_i) = (1, 0)$. Most importantly, in the former case of a quench from $(\gamma_i, h_i) = (1, 0.5)$, we find that the minimum of the Loschmidt echo is not zero in the dynamically disordered phase. In general, for initial conditions (q_i, p_i), the Loschmidt echo (Loschmidt amplitude) vanishes at time t iff $(q(t), p(t)) = (q_i + \pi, -p_i)$. Because the classical motion is restricted to an isoenergetic surface, only states with $H(q(t)p(t)) = H(q_i, p_i)$ are accessible. Hence, in order to have a vanishing Loschmidt echo the condition $H(q_i, p_i) - H(q_i + \pi, -p_i) = -4h_f p_i = 0$ has to be satisfied. Therefore, whenever $h_f p_i \neq 0$, the Loschmidt amplitude has an analytic temporal behaviour (figure 3), even in the case of a quench that crosses a dynamical transition defined through the time-averaged order parameter. This explicitly demonstrates that the two definitions of dynamical phase transitions mentioned in the Introduction are in general unrelated, even in the mean-field limit.

Let us now study the robustness of the zeros of the Loschmidt amplitude when the number of spins N is kept finite, focusing on the short-time dynamics of the fully connected XY model for large but finite N. This can be done either by studying the dynamics of a large spin or by performing a systematic semiclassical expansion using, for example, the positive-P representation [28,29]. This representation is preferred to other phase-space methods in order to avoid the problem of the negative diffusion matrix [28]. We were able to numerically calculate the exact (up to a small statistical error) short-time dynamics, which captures the first minimum of the Loschmidt amplitude. The numerical results thus obtained are plotted in figure 4 and show that the Loschmidt echo approaches the mean-field result as N^{-1}.

Finally, we discuss the stability of the Loschmidt amplitude against quantum fluctuations. The mean-field dynamics is exact in the thermodynamic limit only for long-range models. If we consider the XY model on a cubic lattice with a coordination number Z instead of the infinite-range model, the mean-field solution is only an approximation up to the order $1/Z$. We follow [30] and calculate the first-order quantum corrections to the mean-field. First, we rewrite the Hamiltonian (2.1) using the Fourier transformation

$$H = -\frac{1+\gamma}{2N}\sigma_0^{\mathrm{x}}\sigma_0^{\mathrm{x}} - \frac{1-\gamma}{2N}\sigma_0^{\mathrm{y}}\sigma_0^{\mathrm{y}} - h\sigma_0^{\mathrm{z}} - \frac{1}{N}\sum_{q\neq 0}\Lambda_q\left(\frac{1+\gamma}{2}\sigma_q^{\mathrm{x}}\sigma_{-q}^{\mathrm{x}} + \frac{1-\gamma}{2}\sigma_q^{\mathrm{y}}\sigma_{-q}^{\mathrm{y}}\right) \tag{4.1}$$

with $\sigma_q^a = \sum_R \mathrm{e}^{\mathrm{i}q\cdot R}\sigma_R^a$ and $\Lambda_q = (1/Z)\sum_{\langle a\rangle}\exp(\mathrm{i}qa)$. Then, we assume the following non-vanishing commutation relations up to the leading order in N:

$$[\sigma_0^a, \sigma_0^b] = 2\mathrm{i}\epsilon_{abc}\sigma_0^c, \quad [\sigma_q^a, \sigma_{-q}^b] = 2\mathrm{i}\epsilon_{abc}\sigma_0^c \quad \text{and} \quad [\sigma_q^a, \sigma_0^b] = 2\mathrm{i}\epsilon_{abc}\sigma_q^c. \tag{4.2}$$

We evaluate the equations of motion $\partial_t\sigma_q^a = \mathrm{i}[H, \sigma_q^a]$ assuming (in addition to (4.2)) classical values for $q = 0$ (i.e. $\sigma_0^{\mathrm{x}} = (Nn/2)\sin\theta\cos\phi$, $\sigma_0^{\mathrm{y}} = (Nn/2)\sin\theta\sin\phi$, $\sigma_0^{\mathrm{z}} = (Nn/2)\cos\theta$ with $n \in [0, 1]$, $\phi \in$

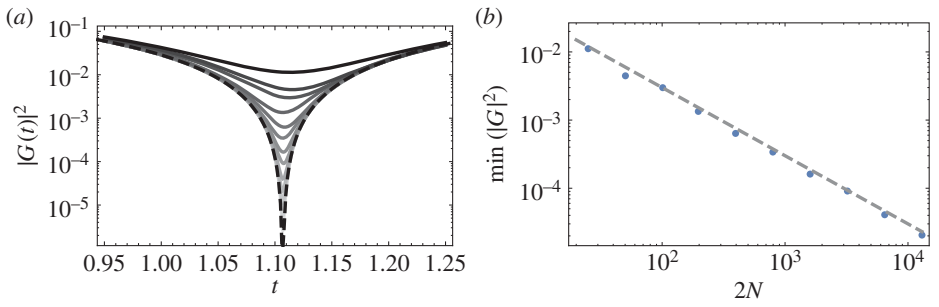

Figure 4. (*a*) Time dependence of the Loschmidt echo around the first minimum for different spin/system sizes (darker lines denote smaller system sizes). The dashed line shows the mean-field result. (*b*) System size dependence of the first minimum of the Loschmidt amplitude shown in (*a*). We use the positive-P representation. The statistical error is of the size of the points in (*b*). The dashed line shows the suggested scaling $\propto N^{-1}$. (Online version in colour.)

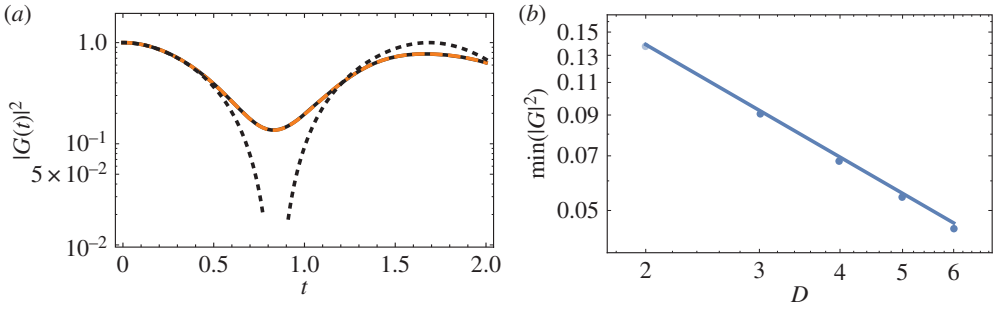

Figure 5. Loschmidt echo around the first minimum. (*a*) Numerical integration including quantum fluctuations for a quench from $(\gamma_i, h_i) = (1, 0)$ to $(\gamma_f, h_f) = (1, 2)$. The dashed line shows the result obtained by the first integration method with $N_{\mathrm{dis}} = 40$ which coincides with the full black line denoting the result obtained by the second integration method with $k_{\max} = 100$. The dashed line shows the mean-field result. (*b*) Dependence of the first minimum of the Loschmidt echo on the coordination number/dimension (for cubic lattice $D = Z/2$). The solid line shows $\propto D^{-1}$ serves as a guide to the eye. (Online version in colour.)

$[0, 2\pi]$ and $\theta \in [0, \pi]$) and defining $C_{ab}(q,t) = \frac{1}{2}\langle \sigma_q^a \sigma_{-q}^b + \sigma_q^b \sigma_{-q}^a \rangle$. This procedure results in a set of coupled differential equations that describe the evolution of $C_{ab}(q,t)$ and of the classical (mean-field) variables. These equations can be solved numerically either by using a uniform discretization in momentum space or by using a new set of variables given by integrals $c_{ab}^{(k)}(t) = \int \mathrm{d}q\, \Lambda_q^k C_{ab}(q,t)$. In the latter case, the time derivatives of the integrated variables of order k can be expressed as a function of integrated variables of orders k and $k+1$; $\partial_t\, c_{ab}^{(k)}(t) = \sum_{cd} f(c_{cd}^{k+1}, c_{cd}^k)$. In order to calculate the time evolution, we truncate this recursion at some finite $k = k_{\max}$. We are interested in the dynamics around the first zero of the Loschmidt echo in the thermodynamic limit. Up to this time, the numerical solution converges quickly with the number of points used in the discretization (first integration method) and agrees with the result obtained using the integrated variables (second integration method, $k_{\max} \approx 100$). The time evolution around the first minimum of the Loschmidt echo is shown in figure 5. We highlight that $|\,G(t)\,|^2$ corrected by quantum fluctuations in the harmonic approximation never vanishes, even when it does at the mean-field level. If $Z \to \infty$, the Loschmidt echo smoothly recovers its mean-field value, actually linearly in $1/Z$ (figure 5). Note that, in contrast with the fate of the zeros in the Loschmidt echo, the mean-field dynamical transition survives the quantum fluctuations (figure 6).

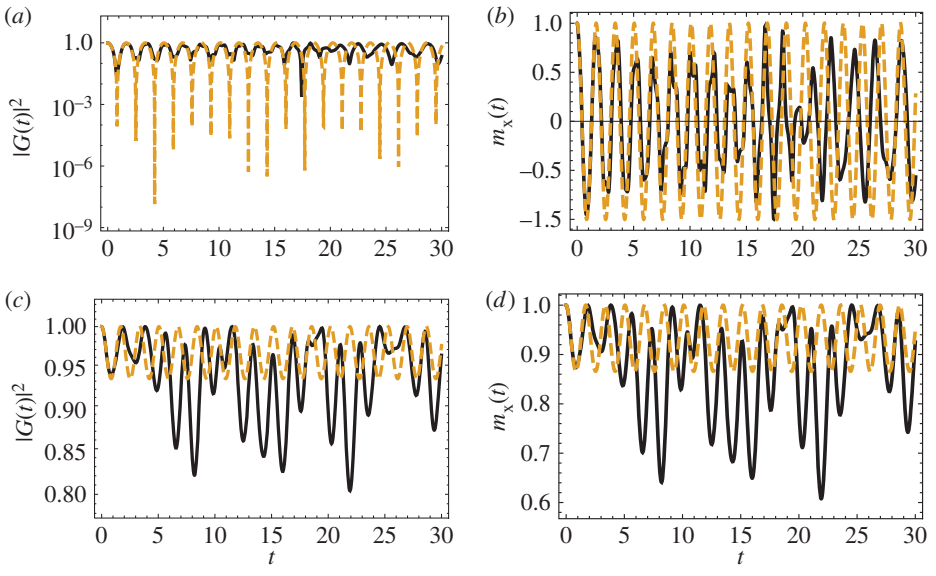

Figure 6. Long-time dynamics of the Loschmidt echo and the m_x. The dashed line represents the mean-field values, the solid line denotes the evolution obtained including first-order quantum correction. We set $D = 2$, $(\gamma_i, h_i) = (1, 0)$ and use integration method 2 with $k_{\max} = 1000$. (*a*,*b*) A quench to the disordered phase $(\gamma_f, h_f) = (1, 2)$, and (*c*,*d*) a quench to the ordered phase $(\gamma_f, h_f) = (1, \frac{1}{2})$. (Online version in colour.)

5. Conclusion

This paper presents a comparison of two different notions of dynamical phase transitions with the equilibrium phase diagram of the infinite-range XY model. We first of all studied the dynamical phase transitions after a quench by computing the time average of the order parameter, showing that the crossing of the equilibrium critical line in a sudden quantum quench starting in the ordered phase does not necessary result in a dynamical phase transition corresponding to a vanishing dynamical order parameter. The dynamical order parameter can be non-vanishing even when the equilibrium-order parameter vanishes at final parameters of the Hamiltonian. Similar behaviour is observed also in the case of the dynamical phase transition determined by the zeros of the Loschmidt amplitude. However, we show that the zeros and non-analyticities in time of the Loschmidt amplitude appear only for particular quenches with $h_f p_i = 0$ and can therefore not be considered as an indicator of a dynamical phase transition in the time-averaged order parameter $\bar{m}_x$. Furthermore, we show that, in contrast to the time-averaged order parameter, the zeros of the Loschmidt amplitude do not survive first-order quantum corrections. In conclusion, the results obtained show that there is no apparent connection between different notions of the dynamical phase transitions encountered in the literature and the equilibrium phase transition in the mean-field XY model.

Authors' contributions. A.S. and M.F. conceived the study; A.S., B.Ž. and M.F. performed the analytical analysis; B.Ž. performed the numerical computations; A.S. drafted the manuscript. All authors gave their approval for publication.

Competing interests. The authors declare that they have no competing interests.

Funding. We received no funding for this study.

Acknowledgements. B.Ž. was supported by Chilean FONDECYT project 3130495.

References

1. Bloch I, Dalibard J, Zwerger W. 2008 Many-body physics with ultracold gases. *Rev. Mod. Phys.* **80**, 885–964. (doi:10.1103/RevModPhys.80.885)

2. Richerme P, Gong Z-X, Lee A, Senko C, Smith J, Foss-Feig M, Michalakis S, Gorshkov AV, Monroe C. 2014 Non-local propagation of correlations in quantum systems with long-range interactions. *Nature* **511**, 198–201. (doi:10.1038/nature13450)
3. Fausti D *et al.* 2011 Light-induced superconductivity in a stripe-ordered cuprate. *Science* **331**, 189–191. (doi:10.1126/science.1197294)
4. Polkovnikov A, Sengupta K, Silva A, Vengalattore M. 2011 *Colloquium*: nonequilibrium dynamics of closed interacting quantum systems. *Rev. Mod. Phys.* **83**, 863–883. (doi:10.1103/RevModPhys.83.863)
5. Berges J, Borsányi S, Wetterich C. 2004 Prethermalization. *Phys. Rev. Lett.* **93**, 142002. (doi:10.1103/PhysRevLett.93.142002)
6. Moeckel M, Kehrein S. 2008 Interaction quench in the Hubbard model. *Phys. Rev. Lett.* **100**, 175702. (doi:10.1103/PhysRevLett.100.175702)
7. Kollar M, Wolf FA, Eckstein M. 2011 Generalized Gibbs ensemble prediction of prethermalization plateaus and their relation to nonthermal steady states in integrable systems. *Phys. Rev. B* **84**, 054304. (doi:10.1103/PhysRevB.84.054304)
8. Marcuzzi M, Marino J, Gambassi A, Silva A. 2013 Prethermalization in a nonintegrable quantum spin chain after a quench. *Phys. Rev. Lett.* **111**, 197203. (doi:10.1103/PhysRevLett.111.197203)
9. Bertini B, Essler FHL, Groha S, Robinson NJ. 2015 Prethermalization and thermalization in models with weak integrability breaking. (http://arxiv.org/abs/1506.02994)
10. Gring M *et al*. 2012 Relaxation and prethermalization in an isolated quantum system. *Science* **337**, 1318–1322. (doi:10.1126/science.1224953)
11. Langen T *et al.* 2015 Experimental observation of a generalized Gibbs ensemble. *Science* **348**, 207–211. (doi:10.1126/science.1257026)
12. Eckstein M, Kollar M, Werner P. 2009 Thermalization after an interaction quench in the Hubbard model. *Phys. Rev. Lett.* **103**, 056403. (doi:10.1103/PhysRevLett.103.056403)
13. Schiró M, Fabrizio M. 2010 Time-dependent mean field theory for quench dynamics in correlated electron systems. *Phys. Rev. Lett.* **105**, 076401. (doi:10.1103/PhysRevLett.105.076401)
14. Sciolla B, Biroli G. 2011 Dynamical transitions and quantum quenches in mean-field models. *J. Stat. Mech., Theor. Exp.* **11**, P11003.
15. Gambassi A, Calabrese P. 2013 Quantum quenches as classical critical films. *Europhys. Lett.* **95**, 66007.
16. Chandran A, Nanduri A, Gubser SS, Sondhi SL. 2013 Equilibration and coarsening in the quantum $o(n)$ model at infinite n. *Phys. Rev. B* **88**, 024306. (doi:10.1103/PhysRevB.88.024306)
17. Sciolla B, Biroli G. 2013 Quantum quenches, dynamical transitions, and off-equilibrium quantum criticality. *Phys. Rev. B* **88**, 201110. (doi:10.1103/PhysRevB.88.201110)
18. Smacchia P, Knap M, Demler E, Silva A. 2014 Exploring dynamical phase transitions and prethermalization with quantum noise of excitations. (http://arxiv.org/abs/1409.1883)
19. Heyl M, Polkovnikov A, Kehrein S. 2013 Dynamical quantum phase transitions in the transverse-field Ising model. *Phys. Rev. Lett.* **110**, 135704. (doi:10.1103/PhysRevLett.110.135704)
20. Andraschko F, Sirker J. 2014 Dynamical quantum phase transitions and the Loschmidt echo: a transfer matrix approach. *Phys. Rev. B* **89**, 125120. (doi:10.1103/PhysRevB.89.125120)
21. Vajna S, Dóra B. 2014 Disentangling dynamical phase transitions from equilibrium phase transitions. *Phys. Rev. B* **89**, 161105. (doi:10.1103/PhysRevB.89.161105)
22. Gambassi A, Silva A. 2011 Statistics of the work in quantum quenches, universality and the critical Casimir effect. (http://arxiv.org/abs/1106.2671)
23. Gambassi A, Silva A. 2012 Large deviations and universality in quantum quenches. *Phys. Rev. Lett.* **109**, 250602. (doi:10.1103/PhysRevLett.109.250602)
24. Vajna S, Dóra B. 2014 Topological classification of dynamical phase transitions. (http://arxiv.org/abs/1409.7019)
25. Canovi E, Werner P, Eckstein M. 2014 First-order dynamical phase transitions. *Phys. Rev. Lett.* **113**, 265702. (doi:10.1103/PhysRevLett.113.265702)
26. Zueco D, Calvo I. 2007 Bopp operators and phase-space spin dynamics: application to rotational quantum Brownian motion. *J. Phys. A, Math. Theor.* **40**, 4635. (doi:10.1088/1751-8113/40/17/015)
27. Klimov AB, Chumakov SM. 2009 *A group-theoretical approach to quantum optics*. Berlin, Germany: Wiley-VCH Verlag.

28. Drummond PD, Gardiner CW. 1980 Generalised p-representations in quantum optics. *J. Phys. A, Math. Gen.* **13**, 2353–2368. (doi:10.1088/0305-4470/13/7/018)
29. Deuar P, Drummond PD. 2002 Gauge *P* representations for quantum-dynamical problems: removal of boundary terms. *Phys. Rev. A* **66**, 033812. (doi:10.1103/PhysRevA.66.033812)
30. Sandri M, Schiro M, Fabrizio M. 2012 Linear ramps of interaction in the fermionic Hubbard model. *Phys. Rev. B* **86**, 075122. (doi:10.1103/PhysRevB.86.075122)